

# Masked Autoencoders in 3D Point Cloud Representation Learning

Jincen Jiang<sup>1</sup>, Xuequan Lu<sup>2</sup>, Lizhi Zhao<sup>1</sup>, Richard Dazaley<sup>2</sup>, and Meili Wang<sup>1</sup>

<sup>1</sup> Northwest A&F University

<sup>2</sup> Deakin University

{jinec,wml}@nwafu.edu.cn; xuequan.lu@deakin.edu.au

**Abstract.** Transformer-based Self-supervised Representation Learning methods learn generic features from unlabeled datasets for providing useful network initialization parameters for downstream tasks. Recently, self-supervised learning based upon masking local surface patches for 3D point cloud data has been under-explored. In this paper, we propose masked Autoencoders in 3D point cloud representation learning (abbreviated as MAE3D), a novel autoencoding paradigm for self-supervised learning. We first split the input point cloud into patches and mask a portion of them, then use our Patch Embedding Module to extract the features of unmasked patches. Secondly, we employ patch-wise MAE3D Transformers to learn both local features of point cloud patches and high-level contextual relationships between patches and complete the latent representations of masked patches. We use our Point Cloud Reconstruction Module with multi-task loss to complete the incomplete point cloud as a result. We conduct self-supervised pre-training on ShapeNet55 with the point cloud completion pre-text task and fine-tune the pre-trained model on ModelNet40 and ScanObjectNN (PB\_T50\_RS, the hardest variant). Comprehensive experiments demonstrate that the local features extracted by our MAE3D from point cloud patches are beneficial for downstream classification tasks, soundly outperforming state-of-the-art methods (93.4% and 86.2% classification accuracy, respectively). *Our source codes will be made publicly available.*

**Keywords:** Self-supervised learning · Point cloud · Completion

## 1 Introduction

Point cloud is a format of 3D data representation, which preserves the geometric information of 3D space, and is widely applied in autonomous driving, virtual reality, remote sensing and many other areas. In recent years, deep learning research on point clouds has developed rapidly, with promising results on tasks such as 3D point cloud shape classification and segmentation [23,33,38,24,9,34,35,32]. However, most existing methods require large labeled 3D point cloud datasets for supervised learning, which are expensive and time-consuming, driving the development of research on unsupervised point cloud learning.

Self-supervised learning is a type of unsupervised learning, i.e., training a neural network with supervisory signals generated by the data itself [16]. As a pioneer of Transformer-based self-supervised pre-training methods, BERT [7] has made remarkable achievements in the field of natural language processing (NLP) by proposing the simple and effective masked language modeling pre-text task, which first randomly masks a portion of tokens within a text and then recovers the masked tokens by the Transformer. Inspired by BERT, several self-supervised vision representation models have been designed. BEiT [2] introduces a masked image modeling task to pre-train the visual Transformer. They tokenize the original input image as discrete visual tokens, and input image patches (some patches are randomly masked) into the Transformer backbone to recover the tokens of masked patches. He *et al.* [13] presents the masked Autoencoders (MAE) method, which randomly masks the patches of the image and inputs the visible patches subset to the encoder to obtain the latent representations, which are then concatenated with the mask tokens and input to the decoder to reconstruct the missing pixels of the original input image.

However, due to the gap between 3D point cloud data and image or text data, BERT-style self-supervised pre-training models for point clouds have not been rarely studied so far. Unlike text data with well-defined language vocabulary, point clouds have no concept of word in the NLP domain for the Transformer’s input unit. A simple idea to follow BERT is to treat each point of the point cloud as a word and treat masked auto-encoding prediction as a regression task, which randomly downsamples the point cloud and predicts the 3D coordinates of each missing point. However, a word in a sentence contains rich information while a single point is unable to provide sufficient information [39]. Similar to the pixel-level recovery task in vision, such a point-wise recovery strategy tends to waste model capability on high-frequency details [26] and fails to learn the local features of the point cloud well. In addition, unlike regular pixels, point clouds have irregular point distributions, and it is more challenging to extract contextual relationships between local patches than image patches with grid structure. Point-BERT [39] makes an attempt to apply the BERT-style model to self-supervised 3D representation learning by devising the Masked Point Modeling (MPM) task to pre-train the Transformer. They propose a point cloud Tokenizer to generate discrete point tokens (i.e. discrete integer number) and divide the point cloud into local patches, which are then randomly masked. The goal of the MPM task is to train the Transformer to recover the initial discrete point tokens of the masked local patches. However, since Point-BERT requires an additional pre-trained Tokenizer, their approach is relatively complicated and time-consuming. In addition, their model cannot learn high-level features directly without the help of MoCo [14] to enhance the feature extraction ability of Transformers.

Motivated by the above analysis, we propose 3D masked Autoencoders (MAE3D), a simple yet effective autoencoding paradigm for 3D point cloud self-supervised representation learning, to conduct the MPM pre-text task. Our MAE3D first splits the input point cloud into patches by k-nearest neighborhood (KNN) algorithm, and mask a portion of these patches, which are subsequently completed.

Our MAE3D consists of three main components: Patch Embedding Module, MAE3D Transformers and Point Cloud Reconstruction Module. We devise the Patch Embedding Module with a patch feature extractor to extract latent representations of visible patches, which are concatenated with positional embedding and fed into MAE3D Transformers to complete the latent representations of masked patches. We then generate the entire point cloud global features by pooling the patch-wise latent representations and feed into our Point Cloud Reconstruction Module using our multi-task reconstruction loss to complete the incomplete point cloud. After the pre-training phase, we load only the pre-trained patch feature extractor of Patch Embedding Module as our pre-trained model and evaluate it with 3D object classification as the downstream task.

The main contributions of this paper are:

1. We propose MAE3D, a novel and effective self-supervised representation learning method for 3D point cloud data.
2. We propose to employ patch-wise MAE3D Transformers to learn both local features of point cloud patches and the high-level contextual relationships between patches through the MPM pre-text task.
3. We design a multi-task reconstruction loss, which considers the predicted center points of all split patches and the completed point cloud.
4. We conduct experiments and results show that our method pre-training on ShapeNet55 and fine-tuning on ModelNet40/ScanObjectNN soundly outperforms state-of-the-art techniques on the classification task, achieving 93.4% and 86.2% classification accuracy, respectively.

## 2 Related Work

### 2.1 Pre-training Transformers

Masked language model (MLM) proposed by BERT [7] discards a portion of the input sequence and trains the model with supervised signals generated from the input sequence itself to recover the missing content. BERT has greatly contributed to the research of pre-training Transformers. Influenced by the successful application of MLM and its variants [17,21] in multilingual language representations pretraining tasks [18,6,18] and large-scale sequence-to-sequence Transformers pretraining tasks [37,25] in the field of NLP, researchers have considered applying the BERT-style model to other areas such as computer vision. ViT [8] replaces the convolutional architectures with the Transformer for the first time to extract image features. ViT splits an image into patches and treats each patch as a word in NLP, and inputs the linear embeddings of these patches into the Transformer for supervised image classification learning. Following BERT, BEiT [2] proposes the masked image modeling (MIM) task for self-supervised visual representation learning. BEiT first takes the discrete VAE [26] as the image tokenizer, which tokenizes the image into discrete visual tokens. In the pre-training phase, BEiT randomly masks a portion of image patches, and feeds these corrupted patches into Transformer to learn to recover the visual tokens of

the original image. More recently, MAE [13] has proposed a more effective asymmetric encoder-decoder architecture for MIM tasks, where the encoder operates on the visible patches to extract the latent representation by a linear projection with concatenated positional embeddings. A lightweight decoder reconstructs the original image from the latent representation and mask tokens.

## 2.2 Supervised point cloud learning

As a pioneer of point-based learning methods that directly consume raw point cloud representation without voxelization or projection, PointNet [23] leverages the symmetry of max-pooling to learn the permutation-invariance features of point clouds. PointNet++ [24] devises a hierarchical architecture that recursively partitions the point cloud to extract local features more effectively, achieving better results than PointNet. DGCNN [33] is a graph-based method that creates a dynamic graph in the feature space and designs EdgeConv to learn the edge features of the graph in each layer. Point Cloud Transformer (PCT) [9] applies the traditional Transformer [31] to point cloud learning by constructing an order-invariant attention mechanism based on the Transformer.

## 2.3 Unsupervised point cloud Learning

Yang *et al.* propose FoldingNet [38], an end-to-end auto-encoder network for unsupervised learning of point clouds. They propose a novel folding-based decoder to transform the 2D grid onto a 3D surface represented by point cloud, achieving low reconstruction errors. MAP-VAE [11] learns global and local features of point clouds by combining global and local self-supervision. LatentGAN [1] proposes a deep Autoencoder architecture to train a minimal GAN in the Autoencoder’s latent space to learn point cloud representations. Jiang *et al.* [15] propose an unsupervised contrast learning method for point clouds. They extract the feature representations of the original point cloud and its transformed version through a shared encoder.

Yu *et al.* [39] propose a BERT-style point cloud self-supervised representation learning model, named Point-BERT, to pre-train Transformer model through MPM task. Following BEiT [2], they require a pre-trained Tokenizer to generate discrete integer number point tokens as a self-supervised signal for training the Transformer. *By contrast, our MAE3D trains the Transformer to directly complete the latent representation of masked patches to reconstruct the point cloud.* In addition, during the fine-tuning phase, Point-BERT loads both the feature extractor network and Transformers, while *we only load the patch feature extractor of Patch Embedding Module as our pre-trained model for downstream tasks*, which makes our architecture more generalizable for different point-based networks and saves computation and storage. Since we do not need a pre-trained Tokenizer, our MAE3D can be more lightweight for pre-training on large-scale datasets.

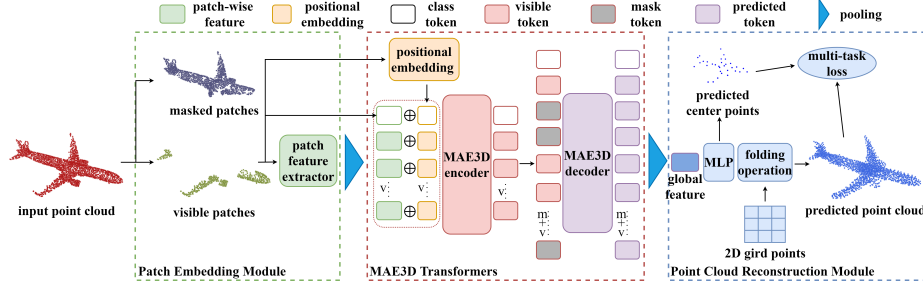


**Fig. 1.** Our MAE3D architecture. The input point cloud is split into patches and mask out a large portion of them. The remaining visible patches are fed to the patch feature extractor to obtain patch-wise features, adding positional embedding and class tokens, then passing them to MAE3D Transformers. The completed global features will be predicted by Transformers and used to reconstruct the point cloud. We develop a multi-task loss to measure both the predicted center points of patches and the reconstructed point cloud.

### 3 Method

Our MAE3D contains three main components: Patch Embedding Module, MAE3D Transformers, and Point Cloud Reconstruction Module. We first pre-train our model with MPM pre-text task, then fine-tune the pre-trained model with 3D object classification as the downstream task to verify its effectiveness. Figure 1 shows the architecture of our work.

#### 3.1 Patch Embedding Module

In this part, we demonstrate the Patch Embedding Module to map the geometric information of the point cloud into latent representations. 3D point clouds are characterized by random order and irregular structure, and the irregularity of the input point clouds is aggravated by masking parts of the point cloud in the MPM pre-text task, which makes it difficult to obtain the embedding features by a simple linear projection as MAE [13] and ViT [8] do for image patches. To complete our MPM pretraining task, we first split point clouds into patches, then randomly mask a portion of them and feed these unmasked patches subset into our patch feature extractor to obtain the patch embedding features.

**Patch split.** We treat the point cloud patch as the word of the BERT-style framework. Given a point cloud  $P \in \mathbb{R}^{N \times 3}$  with  $N$  points, we first uniformly downsample it to a sampled point cloud  $P_c = \{c_i\}_{i=1}^S \in \mathbb{R}^{S \times 3}$  with  $S$  points by farthest point sampling (FPS), where each point in  $P_c$  is used as the center point of a patch. For each point  $c$  in  $P_c$ , we use the KNN algorithm to find a subset of local neighborhood centered on  $c$  from  $P$ , and define all these subsets as point cloud patches  $Q = \{P_i\}_{i=1}^S$ . We try to make these patches cover all points of  $P$  without duplication, i.e.  $Q \approx P$ .

**Masking.** We mask a part of the point cloud patches ( $Q_M = \{P_i\}_{i \in m}$ ,  $m$  is the sequence of the masked patch index) and take these remaining unmasked patches ( $Q_V = \{P_i\}_{i \in v}$ ,  $v$  is the sequence of visible patch index) as input. There are two masking strategies: random masking and block masking. For random masking, we randomly and uniformly select a subset of  $Q$  and remove it. For block masking, we first select a random point  $c_r$  in  $P_c$ , and calculate the K-nearest neighborhood of  $c_r$  from  $P_c$ , then we remove patches in  $Q$  corresponding to the point in that neighborhood. Experimental results of these two strategies can be seen in Section 4.3.

We completed our MPM pre-training task with a high masking ratio, i.e. 0.7, making the task more difficult and challenging, to better learn the latent representations from the unmasked visible patches  $Q_V$ . Meanwhile, a more sparse point cloud input would also make our network more efficient.

An image can be split into a sufficient number of patches, and each of them contains enough pixel information [13]. However, for point clouds, each patch has only a small number of points, e.g. 64 points, and the number of split patches is very limited, e.g., only 32 patches. Therefore, we choose the block masking strategy, which can preserve as much as possible the local spatial structure information of the remaining point cloud with a small number of points, which facilitates the network to obtain its latent representations.

**Patch feature extractor.** Point-based networks, such as PointNet [23] and DGCNN [33], usually include a pooling layer to output global features of a point cloud. The former part before the pooling layer of these networks, i.e. a series of multi-layer perceptions (MLPs), can be naturally treated as the feature extractor  $\Psi(\psi | Q)$  to obtain the latent representations of the input visible patch  $\{\psi_i\}_{i \in v} = \Psi(Q_V)$  in our MAE3D framework. In this case, we can simply use the former part of any point-based network as our feature extractor. In this work, we take the individual patch-wise subsets as input, with the feature extractor capturing the local features of each patch.

### 3.2 MAE3D Transformers

MAE3D is in charge of recovering the latent representations of the missing area of the point cloud and predicting the whole point cloud information (i.e. point cloud global feature) with the limited input. Following the BERT-style manner, in this work, we use the standard Transformer that contains a series of Self-Attention layers and FNN blocks. We use an asymmetric structure, where the encoder focuses on only part of the point cloud (i.e. the visible patch), and the decoder reconstructs the whole point cloud global feature by encoded patches and mask tokens.

**Positional embedding.** The positional embedding allows the operator in Self-Attention layers to well capture the contextual relationships of the input data. In image grids, the embedding of image patches is usually based on the sequence index using a trigonometric-based positional embedding method. However, in 3D data, the coordinates of each point naturally contain information about its position. Therefore, for each point cloud patch, we use its center point

to represent the patch positional information with a trainable embedding layer. All patches' positional embedding can be defined as  $\Phi(c_i) = \{\phi_i\}_{i=1}^S$ . The embedding function  $\Phi$  is an MLP.

**MAE3D encoder.** Our MAE3D encoder is formed by a series of Transformer blocks, and only applied to the visible patch  $Q_V$ . We concatenate the latent representations  $\{\psi_i\}_{i \in v}$  obtained from each visible patch by the patch feature extractor and its positional embedding  $\{\phi_i\}_{i \in v}$  together as the input embedding  $\{x_i\}_{i \in v} = \{\text{concat}(\psi_i, \phi_i)\}_{i \in v}$ . Inspired by ViT [8], we also put a class token  $\Theta_0$  in front of the input sequence, which is formed by a random parameter of trainable vector  $\psi_0$  and a randomly initialized positional embedding  $\phi_0$ , i.e.  $\Theta_0 = \text{concat}(\psi_0, \phi_0)$ . The input to the MAE3D encoder can be denoted as  $\chi = \{\Theta_0, x_i\}_{i \in v}$ , which are then processed through a series of Transformer blocks. Similar to MAE [13], we discard the masked patches directly and do not use any mask tokens in the encoder part, which will save the computational time and memory effectively.

**MAE3D decoder.** For the missing area, we first define mask tokens  $\{\tilde{\xi}_i\}_{i \in m}$  to represent the corresponding masked patch  $Q_M$  that need to be predicted, which consist of a set of randomly initialized learnable latent representations  $\{\tilde{\psi}_i\}_{i \in m}$  and the positional embedding  $\{\phi_i\}_{i \in m}$  of the missing patches. We provide the center point coordinates of each mask patch to compute the corresponding positional embedding, but the true locations of all points in each masked patch are not involved during the whole process. Similarly, we concatenate the initial latent representations and positional embedding to form the mask token as  $\{\tilde{\xi}_i\}_{i \in m} = \{\text{concat}(\tilde{\psi}_i, \phi_i)\}_{i \in m}$ .

Our MAE3D encoder will output the encoded visible patches, called visible tokens  $\{\xi_i\}_{i \in v}$ . Since the MAE3D encoder and decoder have different dimensions, we use a linear layer to match their dimensions. The input to the decoder consists of all patches tokens (i.e. both visible tokens and mask tokens) and class token, which can be defined as  $\Xi = \{\Theta_0, \xi_i, \tilde{\xi}_j\}_{i \in v, j \in m}$ . The decoder has another series of Transformer blocks, and we simply use the standard Transformer following ViT [8] in image tasks. It is worth noting that during the whole process of our MAE3D Transformers, each point cloud patch will be viewed as an individual sample, i.e. MAE3D is a patch-wise approach. The output of the decoder will be a series of feature vectors representing each patch. We concatenate them in the point-wise dimension and then use a pooling layer to fuse the feature vectors into the global feature of the whole point cloud, which will be used for the pre-text task.

### 3.3 Point Cloud Reconstruction Module

The Point Cloud Reconstruction Module is responsible for generating the output point cloud from the global feature. Folding-based methods, like FoldingNet [38] and PCN [40], utilize the folding operation to achieve this task. Motivated by these methods, we develop a patch-based strategy for our MAE3D approach, which can effectively reconstruct the point cloud.



**Patch center prediction.** Similar to PCN [40], we also adopt a series of MLPs to generate a coarse point cloud  $\tilde{P}_c$  as the first step. The MLPs enable better prediction of a sparse set of points to represent the approximate shape of the point cloud. A key point in our method is that this coarse point cloud contains a very small number of points, i.e. 32 points, representing the center of each patch, which correspond to the  $P_c$ . By predicting the center of each patch in the coarse point cloud output, the final reconstructed result will be closer to the ground truth in terms of geometric shape. In other words, the contextual relationships between the patches will be more precise.

**Folding-based patch deformation.** In this part, for the predicted center of each patch, we use 2D grid points (i.e. 8 rows  $\times$  8 colons, totally have 64 points) to generate each point in the patch with folding operation, and the number of each grid will exactly match the real patch. With our improved strategy, we can reduce the computation and storage by avoiding the redundant points generated by PCN [40], and the comparison between the predicted output  $\tilde{P}$  and ground truth  $P$  is much more sensible.

**Reconstruction.** Our MAE3D reconstructs a complete point cloud by predicting the features of each masked patch via inputting portion of the point cloud. With our Point Cloud Reconstruction Module, the predicted global feature of the point cloud can be reconstructed into a point cloud output. Our multi-task reconstruction loss function measures the Chamfer Distance (CD) between the reconstructed point cloud and the original one as well as the predicted center points of patches and the ground truth ones. Unlike MAE [13] that calculates loss only on masked patches, we will compute the loss on the entire point cloud. The Chamfer Distance can be defined as:

$$\text{CD}(S_1, S_2) = \frac{1}{|S_1|} \sum_{x \in S_1} \min_{y \in S_2} \|x - y\|_2^2 + \frac{1}{|S_2|} \sum_{y \in S_2} \min_{x \in S_1} \|y - x\|_2^2, \quad (1)$$

which calculates the average nearest point distance between the predicted point cloud  $S_1$  and the ground truth point cloud  $S_2$ .

Our multi-task loss function uses this metric twice to measure both predicted patch center  $\tilde{P}_c$  and predicted entire point cloud  $\tilde{P}$ , which can be formulated as:

$$L = \text{CD}(\tilde{P}_c, P_c) + \alpha \text{CD}(\tilde{P}, P), \quad (2)$$

where  $\alpha$  is the hyper-parameter representing the weight of the latter term.

### 3.4 Downstream Task

We use 3D object classification as our downstream task in this work to validate the performance of our MAE3D pre-text task pre-training. We take the former part of the backbone network (i.e. the patch feature extractor in Section 3.1) as the pre-trained model which contains valuable parameters. In particular, the local feature and the spatial information of point cloud patches will be of great help for the downstream classification task.



We utilize two schemes to verify the capability of the pre-trained model. The first scheme is to use the pre-trained parameters to initialize the backbone and perform supervised training. The other one is to freeze the pre-trained model so that they will not be trained in the downstream task, and only train a linear classifier to classify the learned representations of this pre-trained model (i.e. self-supervised learning). We will demonstrate the classification results for these two validation schemes in Section 4.

## 4 Experimental Results

### 4.1 Datasets

**Completion pre-training.** We use ShapeNet55 [4] as our pre-training dataset, which has 57,448 models with 55 categories, and all models will be used for the completion task to learn latent features. For each input point cloud, we divide them into 32 point patches which have 64 points for 2,048 points inputs. Then, we choose some patches to be masked with block or random mask sampling strategy. The rest of them, i.e. visible patches, will be used as input to the network.

**Object classification.** We utilize ModelNet40 [35] for 3D object classification. We follow the same data split protocols of previous methods, like PointNet [23] and DGCNN [33]. The dataset contains 9,840 models for training and 2,468 models for testing, which consists of 40 categories. We use 1,024 points with  $(x, y, z)$  normalized positions per model as the input, which is the same as previous works.

We also evaluate our method for the transfer learning on ScanObjectNN dataset [30], which contains 2,902 unique object instances from 15 categories. The objects are real-world point clouds based on the scanned indoor scene data. This dataset poses great challenges for the classification task, due to the involved background and incomplete data. We follow the official data split strategy, and conduct experiments on PB\_T50\_RS which is the most challenging dataset.

### 4.2 Experimental Setting

We use Adam optimizer for all our experiments and implement our work with PyTorch. Unlike DGCNN [33] that uses multiple GPUs, we only use a single RTX TITAN V GPU for training. For the pre-training completion task, we use a batch size of 32 for training. We use the dropouts of 0.5 and the random seed 1, which are the same as DGCNN. The learning rate is set to 0.0001 under the cosine learning scheduler with the 0.0001 weight decay. We train our model for 300 epochs and choose the last checkpoint as our pre-trained model. For downstream 3D object classification on ModelNet40 [35] and ScanObjectNN [30], we set the training batch size to 32 for all experiments. The other settings follow DGCNN.

### 4.3 MAE3D Completion Pre-training

We experiment with the completion of 3D point clouds, which is the pre-text task for our method. Our MAE3D pre-training can be implemented simply and effectively. First, we remove a part of the point cloud by the block masking strategy and use the remaining point cloud as the input of the Patch Embedding Module. Then we predict the latent representation of missing parts by MAE3D Transformers, and finally, fuse the patch-wise features into the global feature to generate the point cloud output using the Point Cloud Reconstruction Module.

We visualize the results of our method in Figure 2. It can be found that the output point cloud can be reconstructed well by our method with only inputting a small part of points. However, certain details in the object can hardly be captured due to the limited input, e.g. in Figure 2, the long strips at the backrest of the chair are recovered as a surface.

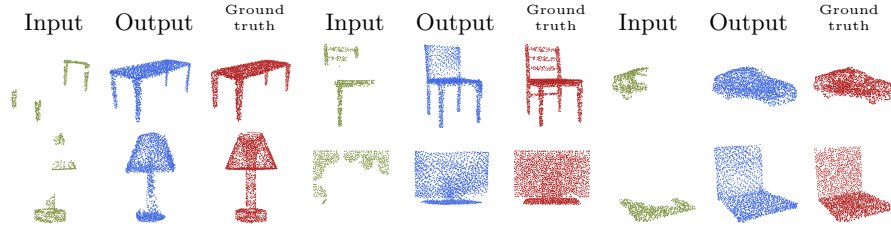


Fig. 2. Sample completion results using our MAE3D with 0.7 block masking ratio.

We also calculate the Chamfer Distance of our MAE3D and some state-of-the-art (SOTA) methods, illustrated in Table 1. To provide a fair comparison, we re-implement and then train two most relevant methods (FoldingNet [38] and PCN [40]) with the same masking strategy and masking ratio, i.e. the input are the same. It can be figured that our MAE3D can obtain the best results, which has the smallest error for the reconstructed output, and the pre-trained model also performs best in fine-tuning downstream task. In addition, we compared our MAE3D with Point-BERT [39], and we use their reported results directly. It is worth mentioning that they input more points, i.e. a smaller masking ratio, and we still outperform them by 0.2% on the downstream classification task.

### 4.4 3D Object Classification

**Pre-training evaluation.** In this experiment, we select PointNet [23] and DGCNN [33] as the backbone, in which the part before the pooling layer is the feature extractor used to obtain the global features of the point cloud. After our MAE3D pre-training, we initialize this part of structure through the pre-trained model. The remaining classification branch (i.e. several MLPs) can be viewed as the projection head, which will be randomly initialized.

**Table 1.** Comparison results of our method and SOTA techniques on the completion task for pre-training (Chamfer Distance) and the classification task for fine-tuning (classification accuracy). DGCNN is used as backbone in our Patch Embedding Module.

Methods	# Points	Masking strategy	Masking ratio	CD ( $\times 10^{-3}$ )	Acc.
FoldingNet [38]	1k	block	0.7	6.858	90.4
PCN [40]	1k	block	0.7	4.394	90.7
Point-BERT [39]	1k	block	[0.25, 0.45]	-	93.2
Point-BERT [39]	1k	block	[0.55, 0.85]	-	92.6
<b>MAE3D</b>	1k	block	0.7	<b>3.127</b>	<b>93.4</b>

As shown in Table 2, the pre-training evaluation based on MAE3D sees a great improvement over the original backbone network, with an increase of 1.4% on PointNet and 0.5% on DGCNN. It is worth noting that MAE3D achieves the best result of 93.4% using DGCNN as the backbone, which exceeds all compared SOTA methods.

**Table 2.** Classification comparison results of our method and supervised methods on ModelNet40.

Methods	Pre-trained	# Points	Acc.
PointNet++ [24]	-	1k	90.7
RSCNN [22]	-	1k	92.9
PointCNN [20]	-	1k	92.5
PointConv [34]	-	1k	92.5
PCT [9]	-	1k	93.2
SO-Net [19]	✓	2k	90.9
3Dpatch [28]	✓	1k	92.4
SSC (RSCNN) [5]	✓	1k	93.0
Point-BERT [39]	✓	1k	93.2
PointNet [23]	-	1k	89.2
MAE3D (PointNet)	✓	1k	90.6 (+1.4)
DGCNN [33]	-	1k	92.9
<b>MAE3D (DGCNN)</b>	✓	1k	<b>93.4 (+0.5)</b>

We also conduct the classification experiment on real-world data, using one of the most challenging variants in ScanObjectNN [30], i.e. PB\_T50\_RS. The result is shown in Table 3, where we can observe that based on our pre-trained model, very strong results of 86.2% can be achieved with fine-tuning, which soundly exceeds the compared SOTA methods. This shows that our method also works very well on real-world data.

**Table 3.** Classification comparison results of our method and supervised methods on ScanObjectNN (PB.T50\_RS).

Methods	Acc.
3DmFV [3]	63.0
PointNet [23]	68.2
SpiderCNN [36]	73.7
PointNet++ [24]	77.9
PointCNN [20]	78.5
BGA (DGCNN) [30]	79.2
BGA (PointNet++) [30]	80.2
Point-BERT [39]	83.1
DGCNN [33]	78.1
<b>MAE3D (DGCNN)</b>	<b>86.2 (+8.1)</b>

**Linear classification evaluation.** To verify that our pre-text task can effectively extract latent representations of point clouds, we use a linear classifier for 3D object classification, which follows the linear protocol on unsupervised learning. The pre-trained model is frozen and used to extract point cloud features, and only the linear classifier is trained.

Table 4 shows the comparison results of our method and the SOTA methods. For a fair comparison, we have classified the experimental results based on the pre-trained dataset. With the reconstruction as the pre-text task, our MAE3D significantly outperforms the other methods with pre-training on ShapeNet55, e.g. exceeding LatentGAN [1] by 6.8% and exceeding FoldingNet [38] by 4.1%.

**Table 4.** Classification comparison results of our method and unsupervised methods on ModelNet40. ShapeNet55 and ModelNet40 pretrained cases are provided.

Methods	Pre-trained dataset	Pre-text task	# Points	Acc.
FoldingNet [38]	ShapeNet55	reconstruction	2k	88.4
VIPGAN [10]	ShapeNet55	reconstruction	2k	90.2
LatentGAN [1]	ShapeNet55	reconstruction	2k	85.7
PointCapsNet [41]	ShapeNet55	reconstruction	2k	88.9
SSC (RSCNN) [5]	ShapeNet55	shape self-correction	2k	92.4
<b>MAE3D (DGCNN)</b>	ShapeNet55	reconstruction	2k	<b>92.5</b>
FoldingNet [38]	ModelNet40	reconstruction	2k	84.4
LatentGAN [1]	ModelNet40	reconstruction	2k	87.3
PointCapsNet [41]	ModelNet40	reconstruction	1k	87.5
MAP-VAE [11]	ModelNet40	reconstruction	2k	90.2
Multi-task [12]	ModelNet40	multiple	2k	89.1
GLR (RSCNN) [27]	ModelNet40	multiple	1k	92.2
<b>MAE3D (DGCNN)</b>	ModelNet40	reconstruction	1k	<b>92.1</b>

#### 4.5 Ablation Studies

**Masking.** In this part, we show the results of two masking strategies with different masking ratios in Figure 3. It can be observed that using block masking can obtain better results in all cases, which has higher accuracy on the classification task. Besides, a high masking ratio, i.e. 0.7, works well on both block masking and random masking. It suggests that the challenge caused by a high masking ratio will benefit the network to capture the latent representations of the sample, which facilitates the classification results. We also calculated the Chamfer Distance for the reconstruction of these two strategies on the ShapeNet55 dataset [4] with the masking ratio of 0.7, and the results are shown in Table 5. It can be seen that block masking still performs better than random masking.

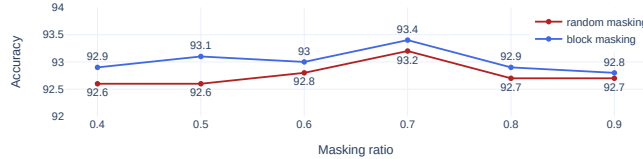


**Fig. 3.** Comparison of different masking strategies and masking ratios on downstream classification task (with DGCNN as the backbone). The y-axis is ModelNet40 testing accuracy (%).

**Table 5.** Comparison results of random masking and block masking. The Chamfer Distance is calculated on ShapeNet55 for pre-training with 0.7 masking ratio.

Masking Strategies	CD ( $\times 10^{-3}$ )
random	3.260
block	<b>3.127</b>

**Training with v.s. without the pre-trained model.** Our pre-trained model can effectively improve the capability of the backbone. It is interesting to find that using our pre-trained parameters as initialization and then fine-tuning on downstream tasks can enable the model to capture the point cloud features at the beginning of the training process. As shown in Figure 4, the case with pre-training achieves better classification performance than training from scratch (i.e. original DGCNN [33]). The model can converge to the optimal solution more efficiently and accurately.

**Pre-training with v.s. without MAE3D Transformers.** We examine whether our MAE3D Transformers can predict the latent representations of the masked patches, i.e. a more complete and significant global feature of the point

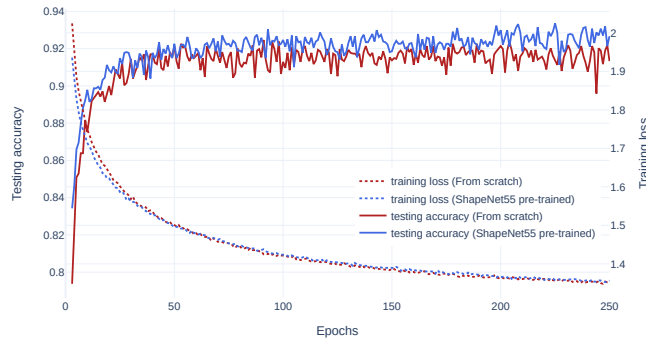


**Fig. 4.** Comparison with or without using pre-trained model for ModelNet40. The y-axes on the left/right are testing accuracy (%) and training loss, respectively.

cloud can be obtained by MAE3D. We perform a comparison experiment to demonstrate this. As shown in Table 6, the network pre-training with MAE3D Transformers can achieve a better result, with a 1% improvement compared to the network without it.

**Table 6.** Comparison results of whether using MAE3D Transformers during pre-training. ShapeNet55 is used for pre-training with block masking and ratio 0.7.

Cases	Acc.
Without MAE3D Transformers	92.4
With MAE3D Transformers	<b>93.4</b>

## 5 Conclusion

In this paper, we proposed MAE3D for point cloud self-supervised representation learning through the MPM pre-text task, which can learn the discriminative features of point cloud patches and the high-level contextual relationships between patches. After pre-training, we load the pre-trained patch feature extractor and fine-tune it on the downstream task of 3D object classification, achieving state-of-the-art accuracy of 93.4% on ModelNet40 and 86.2% on ScanObjectNN (PB\_T50\_RS). This demonstrates the superiority of our proposed method over state-of-the-art methods.

# *Supplementary Material*

Jincen Jiang<sup>1</sup>, Xuequan Lu<sup>2</sup>, Lizhi Zhao<sup>1</sup>, Richard Dazaley<sup>2</sup>, and Meili Wang<sup>1</sup>

<sup>1</sup> Northwest A&F University

<sup>2</sup> Deakin University

{jinec,wml}@nwafu.edu.cn; xuequan.lu@deakin.edu.au

## 1 More Visual Results

### 1.1 Visual Completion Results

We provide more visual results and compare ours with some state-of-the-art (SOTA) methods, like FoldingNet [38] and PCN [40], under the same settings. The average Chamfer Distance for all dataset can be found in the *main manuscript*. Some visual results are shown in Figure 1. Since the point cloud is transformed by data augmentation, for each sample, we provide the different outputs and ground truth corresponding to the input of different transformations. Our MAE3D can predict the masked patches accurately, and the reconstructed point cloud produces the best results among the compared methods. This further confirms that our MAE3D Transformers can obtain better local features of the point cloud patches and therefore our Point Cloud Reconstruction Module can further output more accurate point clouds.

### 1.2 T-SNE Visualization

In Figure 2, we visualize the features that we learned on ModelNet40 [35] with t-SNE visualization. It can be seen that our MAE3D can separate different features relatively well even in the pre-training process, which indicates that our MAE3D Transformers can learn local features among point cloud patches without specific labels. It is interesting to observe that comparing with the original DGCNN [33] (i.e. training from scratch), our MAE3D could enable more separable features after fine-tuning, which implies that our pre-trained model can effectively cope with the downstream classification task.

## 2 Experimental Results on Limited Data

### 2.1 Pre-training Fine-tuning: Few-shot Learning

Following previous work [29], we fine-tune our pre-trained model via few-shot learning. We also use the “ $K$ -way  $N$ -shot” setting, where  $K$  classes are randomly selected from the dataset, and then  $(N + 20)$  samples are chose for each class. Therefore, there are  $K \times (N + 20)$  samples as the sub-dataset, with  $K \times N$  samples as the training set and  $K \times 20$  as the testing set. We adopt the dataset provided



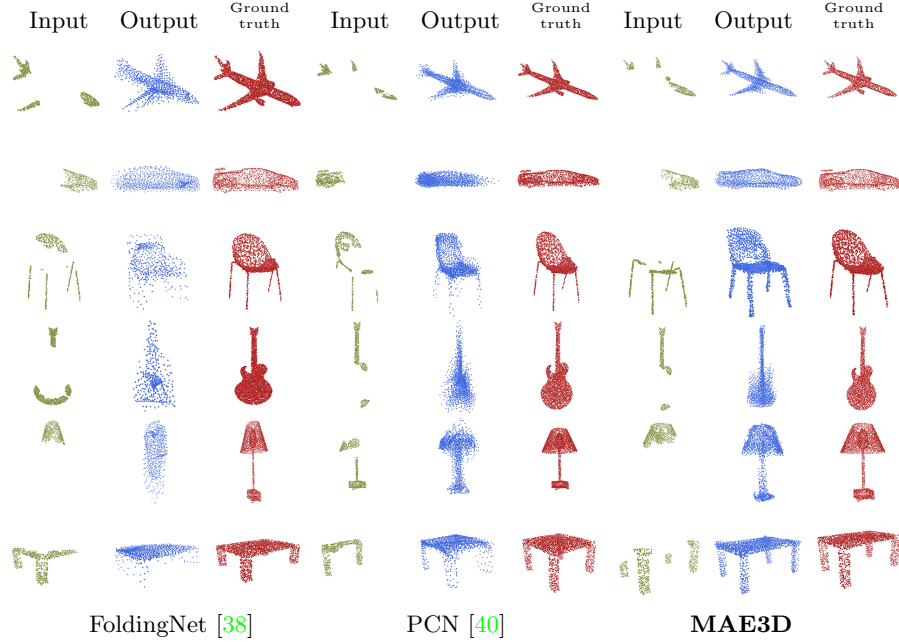


**Fig. 1.** Comparison of sample completion results between our MAE3D and other SOTA methods with 0.7 block masking ratio.

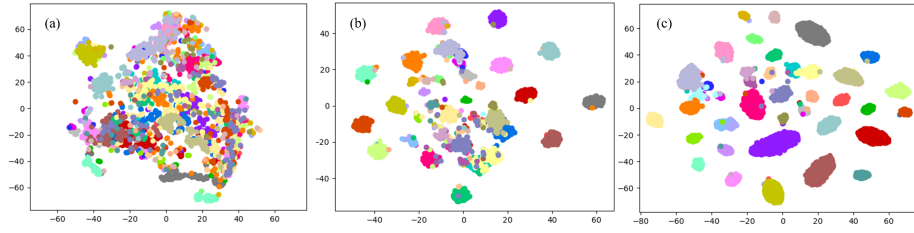


**Fig. 2.** T-SNE visualization of features learned by MAE3D and original DGCNN. (a) MAE3D pre-training, (b) original DGCNN, (c) MAE3D fine-tuning.

by PointBERT [39] to keep the same input as them. In our experiments, we also conduct 10 independent experiments and calculate the mean and the standard deviation over these 10 runs for 4 schemes: “5-way 10-shot”, “5-way 20-shot”, “10-way 10-shot”, and “10-way 20-shot”. The results are shown in Table 1, from which we can see that our MAE3D soundly outperforms PointBERT, indicating that our MAE3D is able to learn sufficient valuable features in a limited dataset.

**Table 1.** Comparison results of few-shot learning on ModelNet40. The mean and standard deviation over 10 independent experiments are shown. The DGCNN’s results are reported in PointBERT.

Methods	5-way 10-shot	5-way 20-shot	10-way 10-shot	10-way 20-shot
DGCNN (rand) [39]	91.8 $\pm$ 3.7	93.4 $\pm$ 3.2	86.3 $\pm$ 6.2	90.9 $\pm$ 5.1
DGCNN (OcCo) [39]	91.9 $\pm$ 3.3	93.9 $\pm$ 3.1	86.4 $\pm$ 5.4	91.3 $\pm$ 4.6
PointBERT [39]	94.6 $\pm$ 3.1	96.3 $\pm$ 2.7	91.0 $\pm$ 5.4	92.7 $\pm$ 5.1
<b>MAE3D</b>	<b>95.2 <math>\pm</math> 3.1</b>	<b>97.9 <math>\pm</math> 1.6</b>	<b>91.1 <math>\pm</math> 4.6</b>	<b>94.2 <math>\pm</math> 3.8</b>

## 2.2 Linear Classifier: Training on Limited Data

We also perform an experiment for training on limited data via linear classifier, and the results can be seen in Table 2. Our MAE3D pre-trained model can achieve 88.3% with DGCNN [33] as the backbone, even with only 20% data for training. Furthermore, in some extreme cases, i.e. using only 1% data, our method also achieves a good result of 61.7%, which exceeds FoldingNet [38] by 5.3%, but is lower than 65.2% of 3DPatch [28]. The reason is that MAE3D removes lots of point cloud patches (with 0.7 masking) during the pre-training, and only learns the features of a limited number of points. When processing the downstream classification task, a very small amount of data will greatly affect the data diversity and result in less improvement of network performance.

**Table 2.** Comparison results of 3D object classification accuracy with limited training data (different ratios). The results without being reported previously are marked as ‘-’.

Methods	1%	2%	5%	10%	20%
FoldingNet [38]	56.4	66.9	75.6	81.2	83.6
3DPatch [28]	<b>65.2</b>	-	-	84.4	-
<b>MAE3D</b>	61.7	<b>69.2</b>	<b>80.8</b>	<b>84.7</b>	<b>88.3</b>

## References

1. Achlioptas, P., Diamanti, O., Mitliagkas, I., Guibas, L.: Learning representations and generative models for 3d point clouds. In: International conference on machine learning. pp. 40–49. PMLR (2018) [4](#), [12](#)
2. Bao, H., Dong, L., Wei, F.: Beit: Bert pre-training of image transformers. arXiv preprint arXiv:2106.08254 (2021) [2](#), [3](#), [4](#)
3. Ben-Shabat, Y., Lindenbaum, M., Fischer, A.: 3dmfv: Three-dimensional point cloud classification in real-time using convolutional neural networks. IEEE Robotics and Automation Letters **3**(4), 3145–3152 (2018) [12](#)
4. Chang, A.X., Funkhouser, T., Guibas, L., Hanrahan, P., Huang, Q., Li, Z., Savarese, S., Savva, M., Song, S., Su, H., et al.: Shapenet: An information-rich 3d model repository. arXiv preprint arXiv:1512.03012 (2015) [9](#), [13](#)
5. Chen, Y., Liu, J., Ni, B., Wang, H., Yang, J., Liu, N., Li, T., Tian, Q.: Shape self-correction for unsupervised point cloud understanding. In: Proceedings of the IEEE/CVF International Conference on Computer Vision. pp. 8382–8391 (2021) [11](#), [12](#)
6. Conneau, A., Khandelwal, K., Goyal, N., Chaudhary, V., Wenzek, G., Guzmán, F., Grave, E., Ott, M., Zettlemoyer, L., Stoyanov, V.: Unsupervised cross-lingual representation learning at scale. arXiv preprint arXiv:1911.02116 (2019) [3](#)
7. Devlin, J., Chang, M.W., Lee, K., Toutanova, K.: Bert: Pre-training of deep bidirectional transformers for language understanding. arXiv preprint arXiv:1810.04805 (2018) [2](#), [3](#)
8. Dosovitskiy, A., Beyer, L., Kolesnikov, A., Weissenborn, D., Zhai, X., Unterthiner, T., Dehghani, M., Minderer, M., Heigold, G., Gelly, S., et al.: An image is worth 16x16 words: Transformers for image recognition at scale. arXiv preprint arXiv:2010.11929 (2020) [3](#), [5](#), [7](#)
9. Guo, M.H., Cai, J.X., Liu, Z.N., Mu, T.J., Martin, R.R., Hu, S.M.: Pct: Point cloud transformer. Computational Visual Media **7**(2), 187–199 (Apr 2021). <https://doi.org/10.1007/s41095-021-0229-5>, <http://dx.doi.org/10.1007/s41095-021-0229-5> [1](#), [4](#), [11](#)
10. Han, Z., Shang, M., Liu, Y.S., Zwicker, M.: View inter-prediction gan: Unsupervised representation learning for 3d shapes by learning global shape memories to support local view predictions. In: Proceedings of the AAAI Conference on Artificial Intelligence. vol. 33, pp. 8376–8384 (2019) [12](#)
11. Han, Z., Wang, X., Liu, Y.S., Zwicker, M.: Multi-angle point cloud-vae: Unsupervised feature learning for 3d point clouds from multiple angles by joint self-reconstruction and half-to-half prediction. In: 2019 IEEE/CVF International Conference on Computer Vision (ICCV). pp. 10441–10450. IEEE (2019) [4](#), [12](#)
12. Hassani, K., Haley, M.: Unsupervised multi-task feature learning on point clouds. In: Proceedings of the IEEE/CVF International Conference on Computer Vision. pp. 8160–8171 (2019) [12](#)
13. He, K., Chen, X., Xie, S., Li, Y., Dollár, P., Girshick, R.: Masked autoencoders are scalable vision learners (2021) [2](#), [4](#), [5](#), [6](#), [7](#), [8](#)
14. He, K., Fan, H., Wu, Y., Xie, S., Girshick, R.: Momentum contrast for unsupervised visual representation learning. In: Proceedings of the IEEE/CVF conference on computer vision and pattern recognition. pp. 9729–9738 (2020) [2](#)
15. Jiang, J., Lu, X., Ouyang, W., Wang, M.: Unsupervised representation learning for 3d point cloud data. arXiv preprint arXiv:2110.06632 (2021) [4](#)

16. Jing, L., Tian, Y.: Self-supervised visual feature learning with deep neural networks: A survey. *IEEE Transactions on Pattern Analysis and Machine Intelligence* **43**(11), 4037–4058 (2021). <https://doi.org/10.1109/TPAMI.2020.2992393> **2**
17. Joshi, M., Chen, D., Liu, Y., Weld, D.S., Zettlemoyer, L., Levy, O.: Spanbert: Improving pre-training by representing and predicting spans. *Transactions of the Association for Computational Linguistics* **8**, 64–77 (2020) **3**
18. Lample, G., Conneau, A.: Cross-lingual language model pretraining. *arXiv preprint arXiv:1901.07291* (2019) **3**
19. Li, J., Chen, B.M., Lee, G.H.: So-net: Self-organizing network for point cloud analysis. In: *Proceedings of the IEEE conference on computer vision and pattern recognition*. pp. 9397–9406 (2018) **11**
20. Li, Y., Bu, R., Sun, M., Wu, W., Di, X., Chen, B.: Pointcnn: Convolution on x-transformed points. *Advances in neural information processing systems* **31** (2018) **11, 12**
21. Liu, Y., Ott, M., Goyal, N., Du, J., Joshi, M., Chen, D., Levy, O., Lewis, M., Zettlemoyer, L., Stoyanov, V.: Roberta: A robustly optimized bert pretraining approach. *arXiv preprint arXiv:1907.11692* (2019) **3**
22. Liu, Y., Fan, B., Xiang, S., Pan, C.: Relation-shape convolutional neural network for point cloud analysis. In: *Proceedings of the IEEE/CVF Conference on Computer Vision and Pattern Recognition*. pp. 8895–8904 (2019) **11**
23. Qi, C.R., Su, H., Mo, K., Guibas, L.J.: Pointnet: Deep learning on point sets for 3d classification and segmentation. In: *Proceedings of the IEEE conference on computer vision and pattern recognition*. pp. 652–660 (2017) **1, 4, 6, 9, 10, 11, 12**
24. Qi, C.R., Yi, L., Su, H., Guibas, L.J.: Pointnet++: Deep hierarchical feature learning on point sets in a metric space (2017) **1, 4, 11, 12**
25. Raffel, C., Shazeer, N., Roberts, A., Lee, K., Narang, S., Matena, M., Zhou, Y., Li, W., Liu, P.J.: Exploring the limits of transfer learning with a unified text-to-text transformer. *arXiv preprint arXiv:1910.10683* (2019) **3**
26. Ramesh, A., Pavlov, M., Goh, G., Gray, S., Voss, C., Radford, A., Chen, M., Sutskever, I.: Zero-shot text-to-image generation (2021) **2, 3**
27. Rao, Y., Lu, J., Zhou, J.: Global-local bidirectional reasoning for unsupervised representation learning of 3d point clouds. In: *Proceedings of the IEEE/CVF Conference on Computer Vision and Pattern Recognition*. pp. 5376–5385 (2020) **12**
28. Sauder, J., Sievers, B.: Self-supervised deep learning on point clouds by reconstructing space. *Advances in Neural Information Processing Systems* **32** (2019) **11, 17**
29. Sharma, C., Kaul, M.: Self-supervised few-shot learning on point clouds. *Advances in Neural Information Processing Systems* **33**, 7212–7221 (2020) **15**
30. Uy, M.A., Pham, Q.H., Hua, B.S., Nguyen, D.T., Yeung, S.K.: Revisiting point cloud classification: A new benchmark dataset and classification model on real-world data. In: *International Conference on Computer Vision (ICCV)* (2019) **9, 11, 12**
31. Vaswani, A., Shazeer, N., Parmar, N., Uszkoreit, J., Jones, L., Gomez, A.N., Kaiser, L., Polosukhin, I.: Attention is all you need. *Advances in neural information processing systems* **30** (2017) **4**
32. Wang, P.S., Liu, Y., Guo, Y.X., Sun, C.Y., Tong, X.: O-cnn. *ACM Transactions on Graphics* **36**(4), 1–11 (Jul 2017). <https://doi.org/10.1145/3072959.3073608>, <http://dx.doi.org/10.1145/3072959.3073608> **1**
33. Wang, Y., Sun, Y., Liu, Z., Sarma, S.E., Bronstein, M.M., Solomon, J.M.: Dynamic graph cnn for learning on point clouds. *ACM Transactions on Graphics (TOG)* (2019) **1, 4, 6, 9, 10, 11, 12, 13, 15, 17**

34. Wu, W., Qi, Z., Fuxin, L.: Pointconv: Deep convolutional networks on 3d point clouds. In: Proceedings of the IEEE/CVF Conference on Computer Vision and Pattern Recognition. pp. 9621–9630 (2019) [1](#), [11](#)
35. Wu, Z., Song, S., Khosla, A., Yu, F., Zhang, L., Tang, X., Xiao, J.: 3d shapenets: A deep representation for volumetric shapes. In: Proceedings of the IEEE conference on computer vision and pattern recognition. pp. 1912–1920 (2015) [1](#), [9](#), [15](#)
36. Xu, Y., Fan, T., Xu, M., Zeng, L., Qiao, Y.: Spidercnn: Deep learning on point sets with parameterized convolutional filters. In: Proceedings of the European Conference on Computer Vision (ECCV). pp. 87–102 (2018) [12](#)
37. Xue, L., Constant, N., Roberts, A., Kale, M., Al-Rfou, R., Siddhant, A., Barua, A., Raffel, C.: mt5: A massively multilingual pre-trained text-to-text transformer. arXiv preprint arXiv:2010.11934 (2020) [3](#)
38. Yang, Y., Feng, C., Shen, Y., Tian, D.: Foldingnet: Point cloud auto-encoder via deep grid deformation (2018) [1](#), [4](#), [7](#), [10](#), [11](#), [12](#), [15](#), [16](#), [17](#)
39. Yu, X., Tang, L., Rao, Y., Huang, T., Zhou, J., Lu, J.: Point-bert: Pre-training 3d point cloud transformers with masked point modeling (2021) [2](#), [4](#), [10](#), [11](#), [12](#), [17](#)
40. Yuan, W., Khot, T., Held, D., Mertz, C., Hebert, M.: Pcn: Point completion network. In: 2018 International Conference on 3D Vision (3DV). pp. 728–737. IEEE (2018) [7](#), [8](#), [10](#), [11](#), [15](#), [16](#)
41. Zhao, Y., Birdal, T., Deng, H., Tombari, F.: 3d point capsule networks. In: Proceedings of the IEEE/CVF Conference on Computer Vision and Pattern Recognition. pp. 1009–1018 (2019) [12](#)